Molecular Vision 2024; 30:290-297 <http://www.molvis.org/molvis/v30/290>
Received 11 August 2023 | Accepted 28 September 2024 | Published 30 September 2024

© 2024 Molecular Vision

Molecular genetic analysis of R124H TGFBIp in one family Avellino corneal dystrophy

Yuluo Huang,[2] Ming Liu,[3] Huayi Lu,[1] Zheng Ji,[2] Tengchuan Jin,[2,4,5,6,7] Shi Lei[1,3]

[1]The First Affiliated Hospital of USTC, Division of Life Sciences and Medicine, University of Science and Technology of China, Hefei, Anhui, P.R. China; [2]Department of Obstetrics and Gynecology, The First Affiliated Hospital of USTC, Division of Life Sciences and Medicine, Center for Advanced Interdisciplinary Science and Biomedicine of IHM, University of Science and Technology of China, Hefei, Anhui, P.R. China; [3]Department of Ophthalmology, Anhui No.2 Provincial People's Hospital, Hefei, China; [4]Laboratory of Structural Immunology, the CAS Key Laboratory of Innate Immunity and Chronic Disease, School of Basic Medical Sciences, Division of Life Sciences and Medicine, University of Science and Technology of China, Hefei, China; [5]Biomedical Sciences and Health Laboratory of Anhui Province, University of Science & Technology of China, Hefei, China; [6]Clinical Research Hospital of Chinese Academy of Sciences (Hefei), University of Science and Technology of China, Hefei, China; [7]Institute of Health and Medicine, Hefei Comprehensive National Science Center, Hefei, Anhui, China

Purpose: The mutation of R124H in TGFBIp causes Avellino corneal dystrophy (ACD, GCD II). However, the molecular mechanisms of ACD caused by the p. R124H mutation are not well understood. In our research, we aimed to explain the molecular mechanisms of ACD caused by the R124H mutation.
Methods: The whole blood of a three-generation family having ACD was studied with the whole exome sequencing. Sanger sequencing was used to identify the mutation gene. The mutant structure of R124H TGFBIp was visualized in Pymol, using the PISA server, Coot and the HDOCK automated docking program. The TGFBIp was expressed in mammalian expression system. And size exclusion chromatography (SEC) was used to identify the aggregate state of TGFBIp.
Results: The whole exome sequencing results showed that there was a c.371G>A mutation in the *TGFBI* gene in one family, including three patients. In biochemical assays, the purified soluble wild-type TGFBIp and R124H TGFBIp formed a homodimer through a novel interface distinct from the previously proposed FAS1–1: FAS1–4 dimer (interface I). R124H TGFBIp is likely to have formed more severe cross-links and aggregation. Therefore, R124H TGFBIp causes homozygous patients to have more serious symptom than heterozygous patients.
Conclusions: In our study, one family having ACD harboring the mutation of R124H TGFBIp was identified. A new homodimerization interface was determined for wild-type TGFBIp and R124H TGFBIp. Besides, we provided a possible molecular explanation for why the symptom of homozygous patients was more severe than those of heterozygous patients. The possible molecular explanation can provide a new insight into the treatment of ACD.

Corneal dystrophy (CD) is a general term for a family hereditary, symmetric, primary and non-inflammatory corneal disease. The characteristics include deposits of different shapes and properties in the corneal tissue that affect the transparency of the cornea and lead to poor vision [1]. CD is caused by mutations in related genes, which leads to the structural or functional damage and has characteristic histopathological changes [2,3]. At present, the related genes which cause CD include the transforming growth factor B-inducing gene (*TGFBI*), *CHST6*, *KRT3*, *COL8A2* etc [4,5]. The inherited patterns of CD comprise autosomal dominant, autosomal recessive and x-linked patterns [6].

The *TGFBI* gene is the first identified and most reported gene related to CD. The *TGFBI* gene is located in zone 1 (5q31), region 3 of the long arm of chromosome 5. It contains a 34,924-nucleotide transcript with 17 exons, and 2052 protein-encoding nucleotide sequence are left after processing [4,7]. The proteins encoded by the *TGFBI* gene are called TGFBIp, collagen fiber-associated protein and corneal epithelin. TGFBIp is involved in the interaction between cells and collagen and plays an important role in cell adhesion.

At present, the types of CD related to the *TGFBI* gene are granular corneal dystrophy type I, Avellino corneal dystrophy (ACD), Reis-Bucklers corneal dystrophy, lattice corneal dystrophy type I, type III A, type I/III A, epithelial basement membrane dystrophy, etc [8]. All of them are the autosomal dominant inheritance, with lattice corneal dystrophy type I and ACD being the most common in China [9]. Until 2020, 74 types of mutations of the *TGFBI* gene have been reported [4]. Among them, the FAS1–1 (amino acid residue 103–236) domain of the *TGFBI* gene is also a mutational hot spot and the R124H mutation is prevalent [10].

Correspondence to: Shi Lei, The First Affiliated Hospital of USTC, Division of Life Sciences and Medicine, University of Science and Technology of China, Hefei, Anhui, 230001, P.R. China; Phone: +86-551-62283120; email: shileidr@outlook.com

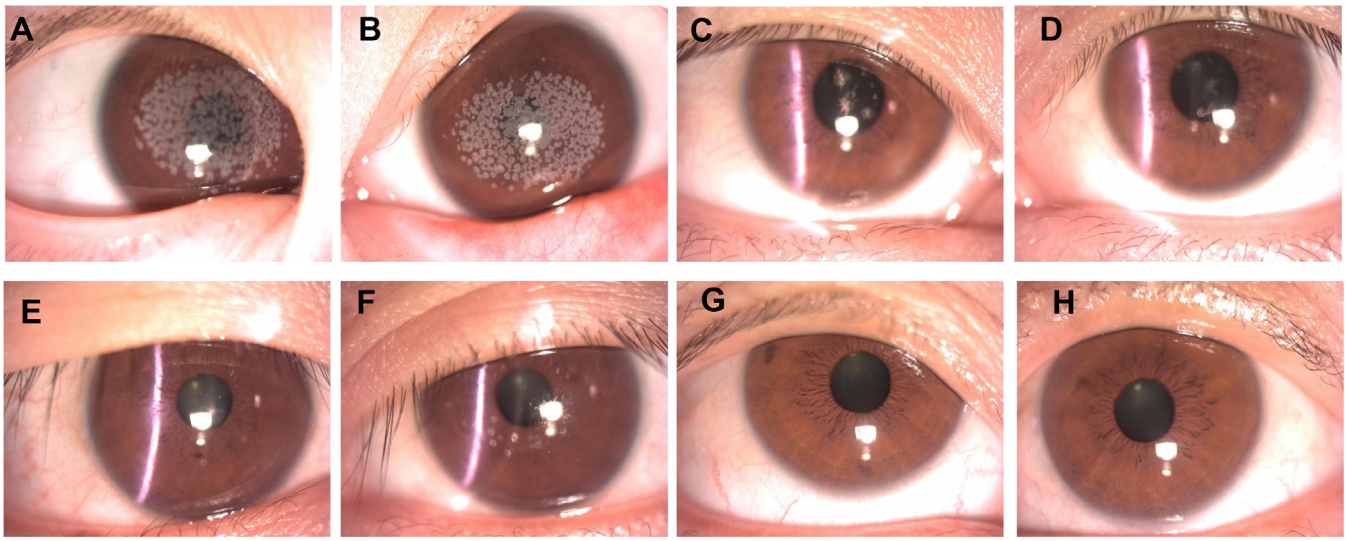

Figure 1. Images of the cornea of three affected family members and one unaffected family member by slit-lamp examination: Corneal image under slit lamp: A, right eye of patient 1, B, left eye of patient 1. C, right eye of patient 2, D, left eye of patient 2. E, right eye of patient 3, F, left eye of patient 3. G, right eye of patient 4, H, left eye of patient 4.

Currently, disease onset of homozygous patients is much earlier than that of heterozygous patients when homozygous patients usually have corneal deposits and visual loss [11]. Heterozygous patients usually have a slow progression of the disease. ACD surgery treatments now include photorefractive keratectomy, laser in situ keratomileusis, and laser epithelial keratomileusis [12]. Some homozygous patients, however, appeared to have recurrence after surgery [13,14]. Moreover, the molecular mechanism of ACD is still unknown, which is particularly important for the treatment of this disease.

In our study, three clinically diagnosed patients with ACD and one subject with a normal phenotype from the same family were used for molecular genetic analysis. The three patients in one family had the same mutation in the *TGFBI* gene. Furthermore, the homotypic interaction interfaces of R124H TGFBIp were studied, which provides useful information for understanding the molecular mechanism of ACD caused by R124H TGFBIp.

METHODS

Clinical evaluations: Our study was reviewed by the First Affiliated Hospital of University of Science and Technology of China Ethics Committee (2022-RE-365) and adhered to the tenets of the Declaration of Helsinki. All subjects were evaluated by fundus examination (Heidelberg Engineering) and slit lamp (ZEISS) examination in clinical inspection. Representative subjects with ACD underwent detailed testing optical coherence tomography (OCT). Some anticoagulated blood was collected from each patient.

Molecular analyses: Anticoagulated blood was tested for whole genome exon sequencing (Novogene Technology Co., Ltd). High-throughput sequencing was used to get raw date. And the Raw data files were converted to sequenced reads by base calling. Validated sequencing data were aligned to the human reference genome (GRch37) by BWA (version 0.7.8-r455). The results of the comparison were called by samtools calling to get the SNP/INDEL information, and ANNOVAR software was used for the final Variation results. Lymphocytes (PBMCs) were separated from the remaining blood samples. PBMCs and plasma were collected and stored at −80 °C.

Sanger sequencing: Genomic DNA was extracted from whole blood with Magen Bio's tissue DNA extraction kits (D3121–02). The genomic DNA was used as a template, then the fourth exon of the *TGFBI* gene was amplified by PCR with the designed primers (Forward primer: agatgcctcctcgtcctct, reveres primer: gtcgactgagcggccgcggtaccaag), and the PCR products were purified by Omega's E.N.Z.A. ®Cycle-Pure-Kit (D6492–02). Purified PCR products were sequenced by the Sanger method.

Structural analysis: According to the R124H mutant structure (PDB code: 7AS7), a head-to-tail interaction interface has been identified through crystal packing analysis, which was displayed in molecular graphic software Coot and Pymol. To simplify the prediction process, we truncated the CROPT-FAS1–1 of R124H TGFBIp as the "head" part and the FAS1–4 of R124H TGFBIp as the "tail" part. Once the "head-to-tail" model was obtained, a docking study was employed to predict

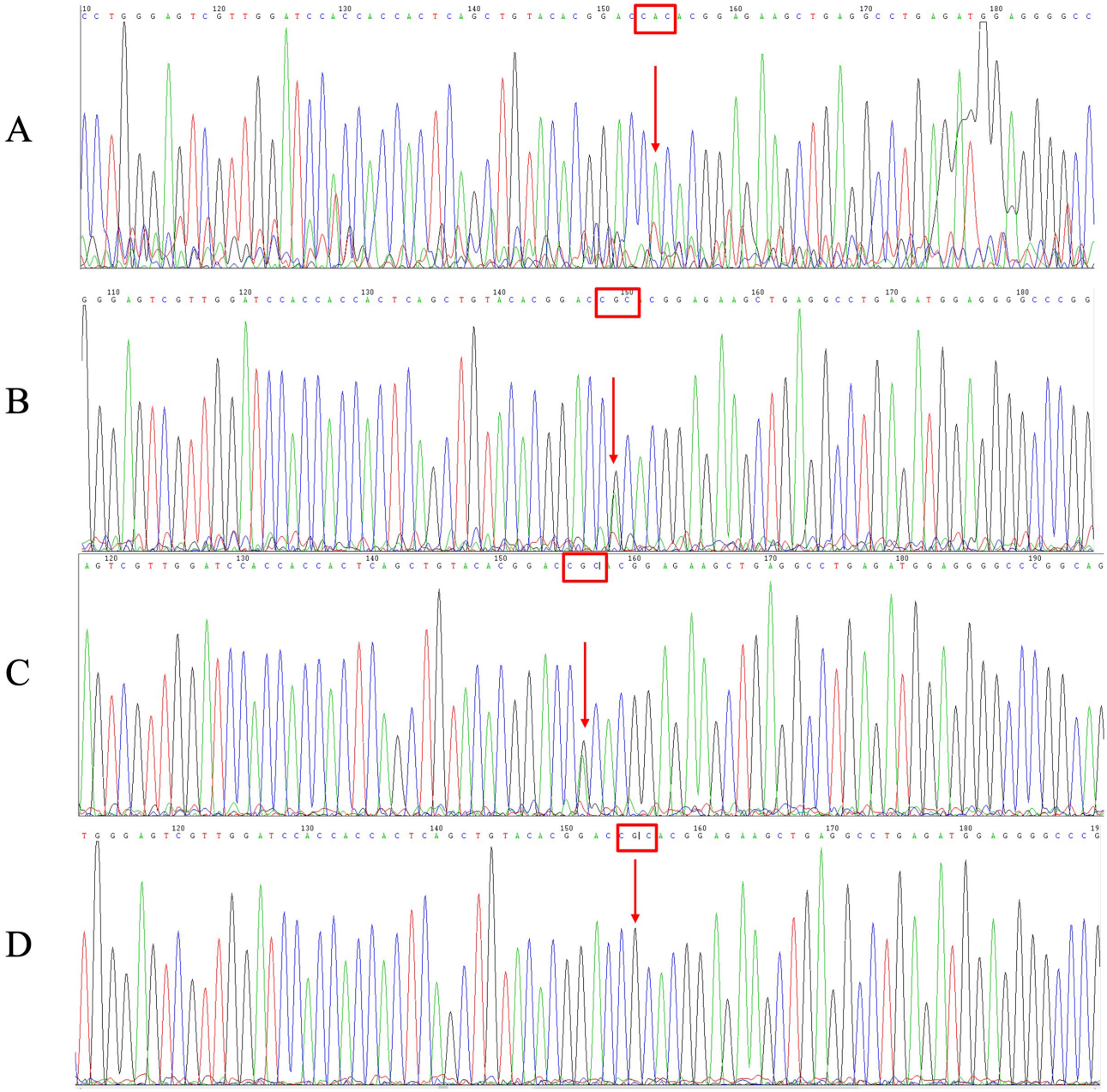

Figure 2. Partial nucleotide sequences of exon 4 of the *TGFBI* gene in affected and unaffected family members.: A, patient 1 had a homozygous mutation of p. R124H in the fourth exon of the *TGFBI* gene; B, Patients 2 had a heterozygous mutation of p. R124H (CGC>CAC) in the fourth exon of the *TGFBI* gene; C, Patient 3 had a heterozygous mutation of p. R124H (CGC>CAC) in the fourth exon of the *TGFBI* gene; D, Patient 4 had no mutation in the fourth exon of the *TGFBI* gene.

the interactions. A non-restricted and template-free docking has been performed with the HDOCK [15] automated docking program. We tested possible docking interfaces in a computer and calculated the binding energy. The wild-type TGFBIp was performed with the same method.

Protein expression and purification: The DNA fragment encoding wild-type human TGFBIp (residues 45–632) was amplified by PCR, and the fragment was ligated into the PTT5 vector with a C-terminal IgG1 Fc tag for expression in HEK293F cells using the polyethylenimine (Polyscience) transfection method. Purification was performed by AKTA

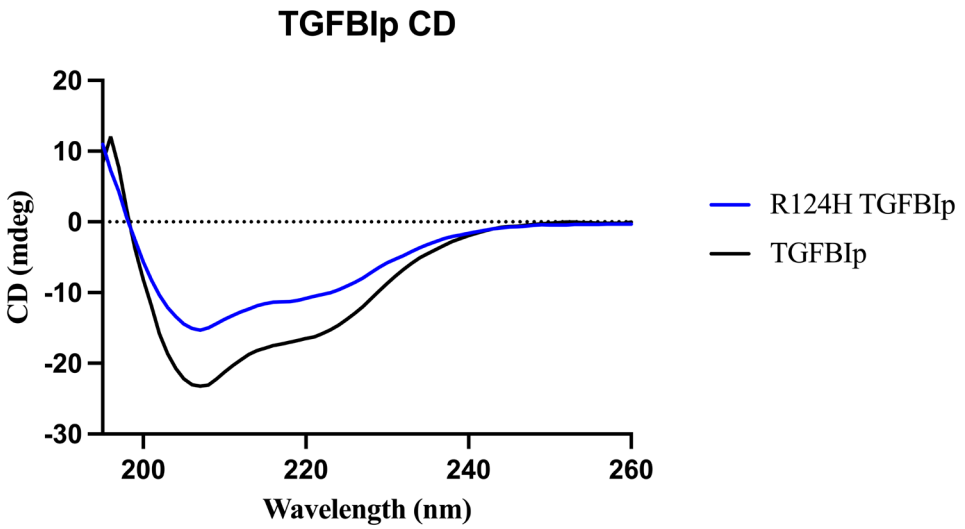

Figure 3. The Wild-type and R124H TGFBIp CD results: The black curve represents wild-type TGFBIp, the blue curve represents R124H mutant TGFBIp.

FPLC. After three days, the medium was harvested for protein purification and added PBS buffer to neutralize the acid produced during the cell culture. The medium was loaded onto a 5 ml-Protein A column (GE Healthcare). Protein was eluted with 0.1M acetic acid. The IgG1 Fc tag was cleaved by overnight TEV protease digestion with dialysis at 4 °C and removed by passing through the Protein A column again. The yield of the sample was assessed by A280 curve. The purity and size of the sample were assessed by SDS–PAGE. The following proteins were prepared using the above method: R124H TGFBIp, R588E TGFBIp and R124H R588E TGFBIp. Meanwhile the oligomerization state of these proteins was evaluated by a Superdex™ 200G 16/600 size exclusion column (GE Healthcare). These proteins were run on non-reduced SDS–PAGE with the same concentration.

Circular dichroism: Protein samples were diluted to 0.15 mg/ml with PBS buffer. Then 400 µl of the sample was added to a 1 mm thick cuvette, and the far-ultraviolet measurements were taken at each integer point from 190 nm to 260 nm at room temperature, and each sample was repeated three times, and the average value was taken for graphing.

RESULTS

Clinical findings: Patient 1, a four-year-old female, had blurred vision in both eyes for one year. Eye examination: the visual acuities of both eyes were 0.1. There was no obvious conjunctival hyperemia in both eyes. In the central 7-mm-diameter area of her left eye (Figure 1A) and her right eye (Figure 1B), gray-white granular turbidity was found with dots and snowflakes. But the intergranular matrix and the peripheral cornea were transparent. And the corneal surface was smooth with an intact epithelial layer (Appendix 1). The diagnosis was severe ACD.

Patient 2, a 30-year-old female, and the mother of patient 1, denied any discomfort in both eyes. Eye examination: the visual acuities of both eyes were 1.0. There was no obvious conjunctival hyperemia in both eyes. In the central 5-mm-diameter area of her left eye (Figure 1C) and her right eye (Figure 1D), gray-white granular turbidity was found with dots and snowflakes. But the intergranular matrix and the peripheral cornea were transparent. And the corneal surface was smooth with an intact epithelial layer (Appendix 1). The diagnosis was mild ACD.

Patient 3, a 30-year-old male, and patient 1's father, denied any discomfort in both eyes. Eye examination: the visual acuities of both eyes were 1.0. There was no obvious conjunctival hyperemia in both eyes. In the central 4-mm-diameter area of his left eye (Figure 1E) and his right eye (Figure 1F), gray-white granular turbidity was found with dots and snowflakes. But the intergranular matrix and the peripheral cornea were transparent. And the corneal surface was smooth with an intact epithelial layer (Appendix 1). Granular turbidity density was similar to patient 2. The diagnosis was mild ACD.

Patient 4, a 58-year-old female, and patient 2's mother, had no symptoms in either eyes. Eye examination: the visual acuities of both eyes were 1.0. There was no obvious conjunctival hyperemia in both eyes. The corneas of her left eye (Figure 1G) and her right eye (Figure 1H) were transparent, and the density of lens was high.

Heterozygocity analysis: According to the correlation between candidate genes and diseases analyzed by the phenolyzer software, fifteen genes related to the occurrence and development of the diagnosis of granular corneal dystrophy are shown in Appendix 2. The range of genetic score is 0–1. The higher the score, the stronger the correlation with the disease. The *TGFBI* gene had the strongest correlation with ACD, whose score was 1. The result of the mutation site screening showed that the Arginine at position 124 had changed to histidine in the fourth exon of the *TGFBI* gene of patient 1, 2 and 3. There was no missense mutation in the *TGFBI* gene in patient 4. The R124H mutation in the fourth exon of the *TGFBI* gene of the three patients led to the occurrence of ACD disease, which was consistent with the clinical diagnosis.

Sanger Sequencing's results showed that patient 1 had a homozygous G to A transversion at position 371 of the *TGFBI* gene. The patients 2 and 3 had a heterozygous G to A change (c.371G > A) in the fourth exon of the *TGFBI* gene, modifying the arginine codon into histidine at position 124 (Figure 2).

Molecular interface analysis: Nielsen et al. had found that the mutation R124H can cause the H124 residue of one TGFBIp molecule to interact with the R555 residue of another TGFBIp molecule through hydrogen bonding [16]. This interaction formed a new dimerization interface I, which does not exist in wild-type TGFBIp. The docking of both wild-type and R124H mutants produced identical interface I, as observed in the crystal packing of the R124H crystal structure. We selected the 20 values with the largest absolute values of ability scores for graphical analysis (RMSD <5 Å). Binding energy scores for the R124H mutant range from −170 to −201, while scores of wild-type range from −126 to −175 (Appendix 3). The higher absolute value of binding energy scores, the stronger interaction between proteins. It is indicated that the R124H mutation favors the head-to-tail interaction mediated by interface I. The absolute value of binding energy scores is positively related to the stability of the structure. The docking result showed that R124H TGFBIp can form interface I but not wild-type TGFBIp.

Possible mechanism of disease pathogenesis: Having identified the critical mutation sequence that leads to the disease,

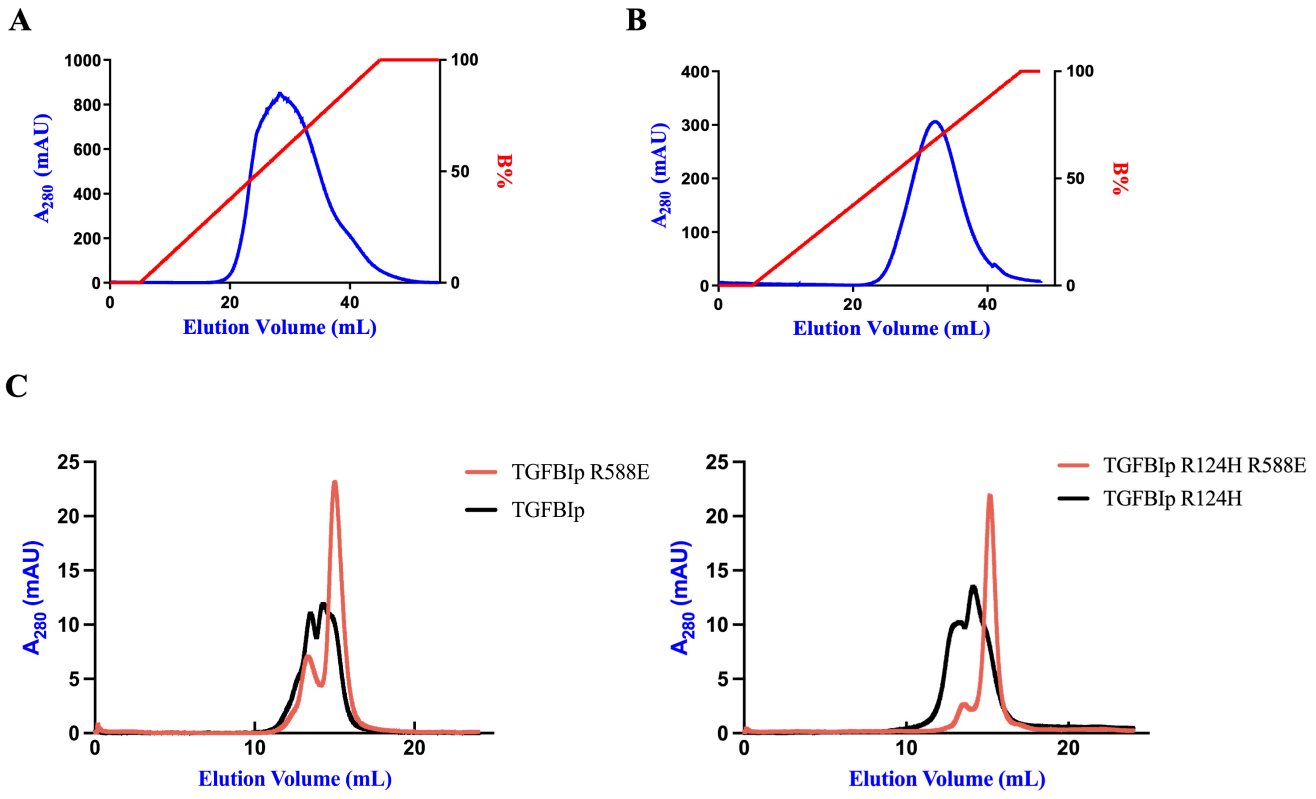

Figure 4. R588 is important to the Wild-type and R124H TGFBIp dimerization. **A**: Size exclusion chromatograph of the Wild-type TGFBIp. **B**: Size exclusion chromatograph of the R124H TGFBIp. **C**: Wild-type TGFBIp and R588E TGFBIp at concentration 14 μM were collected to calibrated SEC. **D**: R124H TGFBIp and R124H R588E TGFBIp at concentration 14 μM were collected to calibrated SEC.

we sought to understand the mechanism that causes such clinical symptoms. By analyzing the interface I in the TGFBIp R124H mutant crystal, docking results supported the idea that such an interaction is unfavorable for the wild-type protein.

To explore the details of homotypic interactions of wild-type TGFBIp protein, the aggregation state of the R124H mutant in solution and its major homotypic interfaces were analyzed by PISA server. The result showed that R124H TGFBIp was likely to exist as dimers in solution (Appendix 4). It is important that this dimerization interface was distinguished from the previously identified head-to-tail interface (interface I) that was created by the R124H mutation, and we named it interface II. There were nine hydrogen bonds and two salt bridges in the interface II. Among them, R588 formed a salt bridge with E89.

Even though wild-type proteins analyzed by PISA server failed to form dimerization of the interface II, we proposed that the interface II mediated the homotypic interaction for both wild-type TGFBIp and R124H TGFBIp based on its favorable properties. To verify our hypothesis of a homotypic interface, wild-type TGFBIp, R124H TGFBIp, a charge reversion mutant at the interface II (R588E) TGFBIp, and R124H R588E TGFBIp were expressed. The wild-type protein and the three mutant proteins have the same negative peaks at 208 nm and 222 nm, along with a positive peak at about 195 nm. This indicates that the secondary structures of both wild-type TGFBIp and R124H TGFBIp are formed by a combination of α-helix and β-folding (Figure 3). The pathogenic mutations did not disrupt the overall secondary structure of TGFBIp. The chromatographic results of proteins purification were shown in Figure 4A,B. The same number of cells from the same batch were used to express and purify the proteins at the same time, and it was found that the yield of the R124H protein was more than the wild-type protein. This suggests that the R124H mutation may affect protein expression yield. When analyzing protein polymerization states with SEC, the wild-type TGFBIp and R124H TGFBIp mostly existed as a dimer. While for the R588E mutants, the proteins existed largely as monomers (Figure 4C), which supported our hypothesis of interface II.

Furthermore, the non-reduced SDS–PAGE result (Figure 5) shows that the R124H mutation caused more disulfide bond formation, which may also have contributed to disease pathogenesis.

DISCUSSION

In our study, we found that the clinical severity of homozygous patients was much greater than that of heterozygous patients. To investigate the mechanism of ACD, anticoagulated blood was tested for whole exome sequencing. The three patients had a G to A transition in the fourth exon of the *TGFBI* gene. To study the properties of TGFBIp, the proteins were expressed in mammalian system. It was found that the yield of R124H mutant protein was lower than that of the wild-type protein, which indicated that the mutant protein may have other influences during the expression and secretion

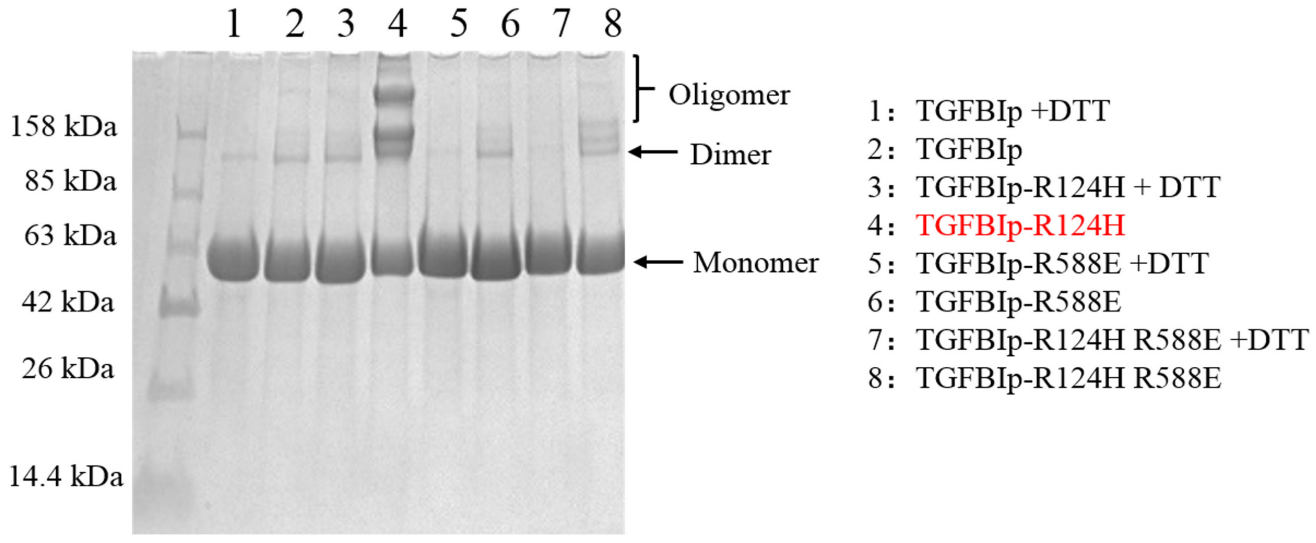

Figure 5. R124H mutation caused more disulfide bond formation: The protein samples of add DTT and without DDT were used to run on SDS–PAGE. The SDS–PAGE analysis of TGFBIp and mutant TGFBIp.

process. Nielsen et.al found that the R124H mutation created a head-to-tail dimerization interface I, which was unfavorable for wild-Type TGFBIp [16]. This result was in agreement with our docking analysis. Besides, we discovered a new dimerization interface II by PISA server and found that the interface II existed in both wild-type and R124H mutation proteins. We verified the existence of interface II by designing mutations in R588E. Based on the R588 forms a salt bridge with E89 in the binding interface II, the mutation of R588E alters the amino acid charge at 588 and disrupts the formation of interface II. This suggests that the interaction of R588 with E89 maybe is important for the existence of interface II. The non-reduced SDS–PAGE result also certified that the R124H TGFBIp enhanced self-association.

To sum up, we concluded that the R124H mutant made the protein susceptible to form aggregate and decreased the solubility of the TGFBIp in the cornea. When mutants occur, homozygous patients harboring the R124H mutation may have more mutant protein precipitation in the cornea, and their symptoms are more severe. Due to the steric hindrance and charge repulsion [16], less R124H TGFBIp precipitation forms in heterozygous patients, which leads to delayed and mild disease pathogenesis. The results suggest that reducing the amount of mutant protein can alleviate the occurrence of disease and provide a potential treatment strategy for ACD.

There are other mechanisms for ACD. The mutation of R124H will cause the abnormal redistribution of TGFBIp into the lysosome [17,18]. Even if the structure of TGFBIp is not damaged, mutations in the FAS1–1 domain may still affect the interaction between TGFBIp and the extracellular proteins. The R124H mutation disrupted the interaction of periostin and TGFBIp [19]. It has been found that the abnormal combination of periostin and TGFBIp is very important to the occurrence of ACD.

Conclusions: In summary, a non-synonymous SNP associated with ACD was studied in this paper. Patient 1 had ACD caused by a homozygous G to A transversion at position 371 in the *TGFBI* gene. A new dimer interface II was discovered in wild-type TGFBIp and R124H TGFBIp. Moreover, the possible mechanism by which homozygous patients have more serious symptoms than heterozygous patients was explained.

APPENDIX 1. IMAGES OF THE CORNEA OF THREE AFFECTED FAMILY MEMBERS BY OCT:

To access the data, click or select the words "Appendix 1." A, right eye of patient 1 (upper), left eye of patient 1 (bottom). B, right eye of patient 2(upper), left eye of patient 2 (bottom). C, right eye of patient 3 (upper), left eye of patient 3.

APPENDIX 2. EXON SEQUENCING RESULTS.

To access the data, click or select the words "Appendix 2." Phenolyzer software was used to sort the analyzed candidate genes and obtain candidate genes related to disease.

APPENDIX 3. THE DOCKING ENERGY OF R124H TGFBIP AND R124H TGFBIP:

To access the data, click or select the words "Appendix 3." Selecting twenty binding energy score. Statistical analysis: two-tailed t text, $p<0.0001$.

APPENDIX 4. THE INTERFACE II OF R124H TGFBIP:

To access the data, click or select the words "Appendix 4." The PISA analysis of interface II of R124H TGFBIp and some residues of interface II.

ACKNOWLEDGMENTS

This study was supported by the Strategic Priority Research Program of the Chinese Academy of Sciences (Grant No. XDB0490000), the National Key Research and Development Program of China (Grants No. 2022YFC2304102 and 2022YFC2303300). Declaration of interest statement: The author declares no competing interests. Data availability statement: The data used to support the findings of this study were supplied by Tengchuan Jin under license and so cannot be made freely available. Requests for access to these data should be made to Tengchuan Jin. Dr. Tengchuan Jin (Jint@ustc.edu.cn) and Dr. Shi Lei (shileidr@outlook.com) are co-corresponding authors for this study.

REFERENCES

1. Kheir V, Cortés-González V, Zenteno JC, Schorderet DF. Mutation update: TGFBI pathogenic and likely pathogenic variants in corneal dystrophies. Hum Mutat 2019; 40:675-93. [PMID: 30830990].

2. García-Castellanos R, Nielsen NS, Runager K, Thøgersen IB, Lukassen MV, Poulsen ET, Goulas T, Enghild JJ, Gomis-Rüth FX. Structural and Functional Implications of Human Transforming Growth Factor β-Induced Protein, TGFBIp, in Corneal Dystrophies. Structure 2017; 25:1740-1750.e2. [PMID: 28988748].

3. Choi S-I, Kim B-Y, Dadakhujaev S, Oh J-Y, Kim T-I, Kim JY, Kim EK. Impaired autophagy and delayed autophagic clearance of transforming growth factor β-induced protein (TGFBI) in granular corneal dystrophy type 2. Autophagy 2012; 8:1782-97. [PMID: 22995918].

4. Nielsen NS, Poulsen ET, Lukassen MV, Chao Shern C, Mogensen EH, Weberskov CE, DeDionisio L, Schauser L,

Moore TCB, Otzen DE, Hjortdal J, Enghild JJ. Biochemical mechanisms of aggregation in TGFBI-linked corneal dystrophies. Prog Retin Eye Res 2020; 77:100843[PMID: 32004730].

5. Klintworth GK. Corneal dystrophies. Orphanet J Rare Dis 2009; 4:7-[PMID: 19236704].

6. Boutboul S, Black GCM, Moore JE, Sinton J, Menasche M, Munier FL, Laroche L, Abitbol M, Schorderet DF. A subset of patients with epithelial basement membrane corneal dystrophy have mutations in TGFBI/BIGH3. Hum Mutat 2006; 27:553-7. [PMID: 16652336].

7. Klintworth GK, Bao W, Afshari NA. Two mutations in the TGFBI (BIGH3) gene associated with lattice corneal dystrophy in an extensively studied family. Invest Ophthalmol Vis Sci 2004; 45:1382-8. [PMID: 15111592].

8. Kannabiran C, Klintworth GK. TGFBI gene mutations in corneal dystrophies. Hum Mutat 2006; 27:615-25. [PMID: 16683255].

9. Yang J, Han X, Huang D, Yu L, Zhu Y, Tong Y, Zhu B, Li C, Weng M, Ma X. Analysis of TGFBI gene mutations in Chinese patients with corneal dystrophies and review of the literature. Mol Vis 2010; 16:1186-93. [PMID: 20664689].

10. Runager K, Basaiawmoit RV, Deva T, Andreasen M, Valnickova Z, Sørensen CS, Karring H, Thøgersen IB, Christiansen G, Underhaug J, Kristensen T, Nielsen NC, Klintworth GK, Otzen DE, Enghild JJ. Human phenotypically distinct TGFBI corneal dystrophies are linked to the stability of the fourth FAS1 domain of TGFBIp. J Biol Chem 2011; 286:4951-8. [PMID: 21135107].

11. Okada M, Inoue SYY, Watanabe H, Maeda N, Shimomura Y, Ishii Y, Tano Y. Severe corneal dystrophy phenotype caused by homozygous R124H keratoepithelin mutations. IOVS 1997; 39:1947-53. .

12. Han KE, Kim TI, Chung WS, Choi SI, Kim BY, Kim EK. Clinical findings and treatments of granular corneal dystrophy type 2 (avellino corneal dystrophy): a review of the literature. Eye Contact Lens 2010; 36:296-9. [PMID: 20724852].

13. Kim T. Comparison of corneal deposits after LASIK and PRK in eyes with granular corneal dystrophy type II. Refract Surg. 2008; 24:392-5. .

14. Lee JH. Exacerbation of granular corneal dystrophy type II (Avellino corneal dystrophy) after LASEK. J Refract Surg 2008; 24:39-45. .

15. Yan Y, Tao H, He J, Huang S-Y. The HDOCK server for integrated protein-protein docking. Nat Protoc 2020; 15:1829-52. [PMID: 32269383].

16. Nielsen NS, Gadeberg TAF, Poulsen ET, Harwood SL, Weberskov CE, Pedersen JS, Andersen GR, Enghild JJ. Mutation-induced dimerization of transforming growth factor-β-induced protein may drive protein aggregation in granular corneal dystrophy. J Biol Chem 2021; 297:100858[PMID: 34097874].

17. Choi SI, Maeng YS, Kim TI, Lee Y, Kim YS, Kim EK. Lysosomal trafficking of TGFBIp via caveolae-mediated endocytosis. PLoS One 2015; 10:e0119561[PMID: 25853243].

18. Han KE, Choi SI, Kim TI, Maeng YS, Stulting RD, Ji YW, Kim EK. Pathogenesis and treatments of TGFBI corneal dystrophies. Prog Retin Eye Res 2016; 50:67-88. [PMID: 26612778].

19. Kim B-Y, Olzmann JA, Choi SI, Ahn SY, Kim TI, Cho H-S, Suh H, Kim EK. Corneal dystrophy-associated R124H mutation disrupts TGFBI interaction with Periostin and causes mislocalization to the lysosome. J Biol Chem 2009; 284:19580-91. [PMID: 19478074].

Articles are provided courtesy of Emory University and The Abraham J. & Phyllis Katz Foundation. The print version of this article was created on 30 September 2024. This reflects all typographical corrections and errata to the article through that date. Details of any changes may be found in the online version of the article.